Electronic Supplementary Information (ESI)

How similar is similar? Exploring the binary and ternary solid solution landscapes of *p*-methyl/chloro/bromo-benzyl alcohols.

A. K. S. Romasanta,[a] D. Braga,[a] M. T. Duarte[b] and F. Grepioni[a]

[a] *Dipartimento di Chimica G. Ciamician, University of Bologna, Via Selmi 2, 40126 Bologna, Italy*
[b] *Centro de Química Estrutural, Departamento de Engenharia Química e Biológica, Instituto Superior Técnico, Av. Rovisco Pais 1, Lisbon, Portugal*

ESI-Table 1. Single crystal data collected at room temperature for the *p*-$Me_{0.5}Br_{0.5}BA$ solid solution and for *p*-BrBA.

	p-$Me_{0.5}BABr_{0.5}BA$	*p*-$Cl_{0.5}BABr_{0.5}BA$	*p*-BrBA
Formula	$C_{7.5}H_{8.5}Br_{0.5}O$	$C_7H_7Br_{0.5}Cl_{0.5}O$	C_7H_7BrO
fw	154.60	164.81	187.04
Cryst. System	monoclinic	monoclinic	monoclinic
space group	$P2_1$	$P2_1$	$P2_1$
Z	2	2	2
a (Å)	6.044(2)	5.9892(6)	6.0614(5)
b (Å)	4.974(1)	4.9395(5)	4.9572(4)
c (Å)	12.231(5)	12.086(1)	12.1601(10)
α (deg)	90.0	90.0	90.0
β (deg)	103.69(4)	102.59(1)	102.523(8)
γ (deg)	90.0	90.0	90.0
V (Å^3)	357.2(2)	348.94(6)	356.69(5)
D_{calc} (g/cm^3)	1.437	1.569	1.741
μ (mm^{-1})	2.869	3.127	5.673
Measd reflns	1188	1560	1556
Indep reflns	904	1206	1244
R1[on F_0^2, I>2σ(I)]	0.0943	0.0512	0.0480
wR2 (all data)	0.2507	0.1232	0.1165

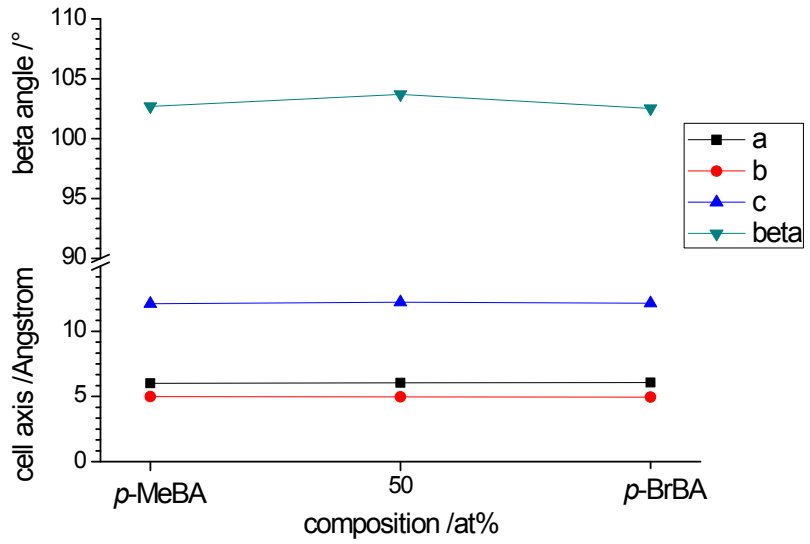

Scheme ESI-1. Comparison of cell parameters for pure *p*-MeBA, *p*-$Me_{0.5}BABr_{0.5}BA$ and *p*-BrBA.

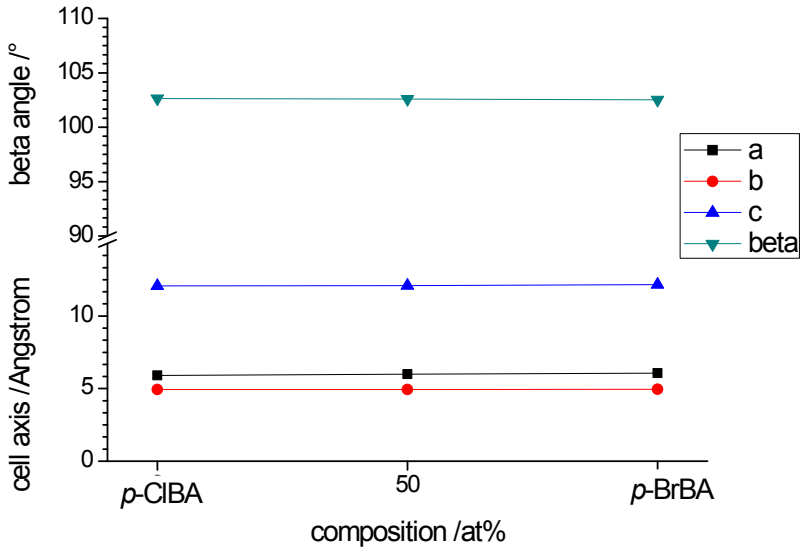

Scheme ESI-2. Comparison of cell parameters for pure *p*-ClBA, *p*-$Cl_{0.5}BABr_{0.5}BA$ and *p*-BrBA.

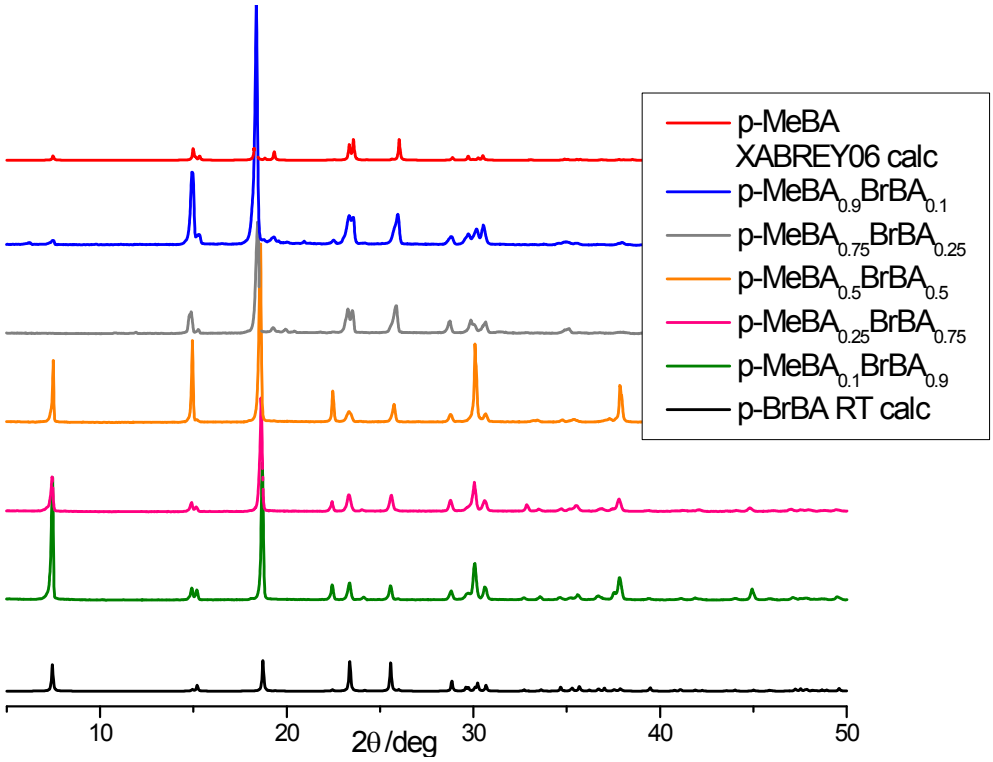

Fig. ESI-1. Comparison of X-ray powder patterns for *p*-$MeBA_{1-x}BrBA_x$ solid solutions. From top: x = 0 [*p*-MeBA (XABREY06) at RT], 0.1, 0.25, 0.5, 0.75, 0.9, 1.0 (*p*-BrBA, RT, calc.).

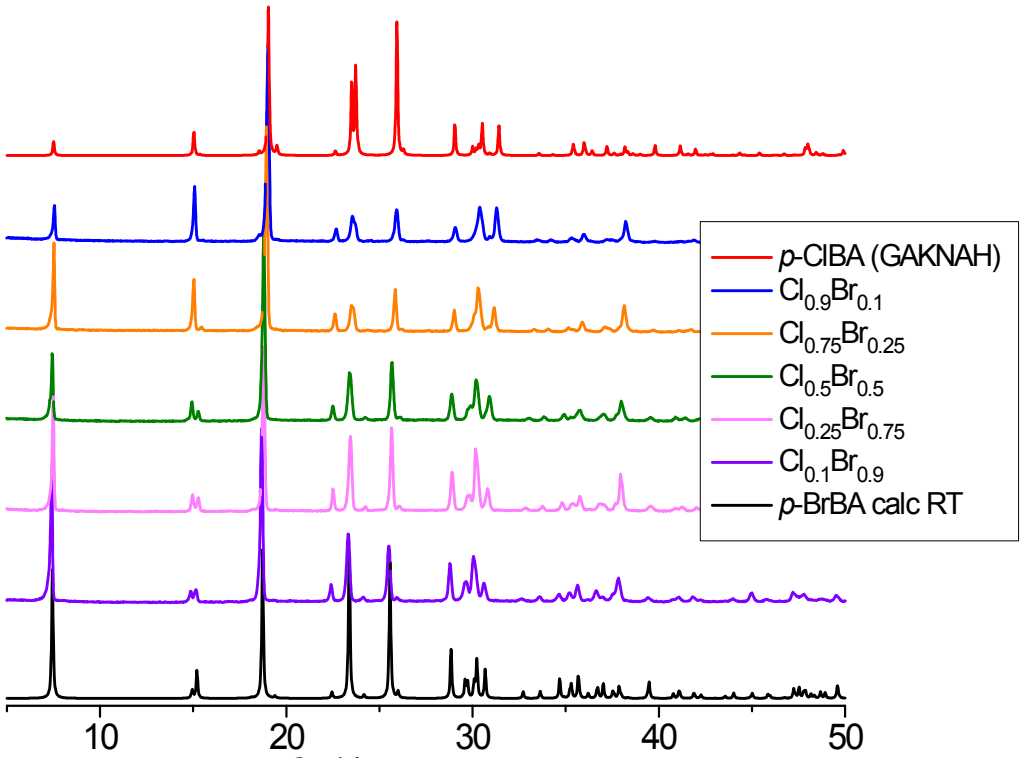

Fig. ESI-2. Comparison of X-ray powder patterns for $ClBA_{1-x}BrBA_x$ solid solutions. From top: x = 0 [*p*-ClBA (GAKNAH) at RT], 0.1, 0.25, 0.5, 0.75, 0.9, 1.0 (*p*-BrBA, RT, calc.).

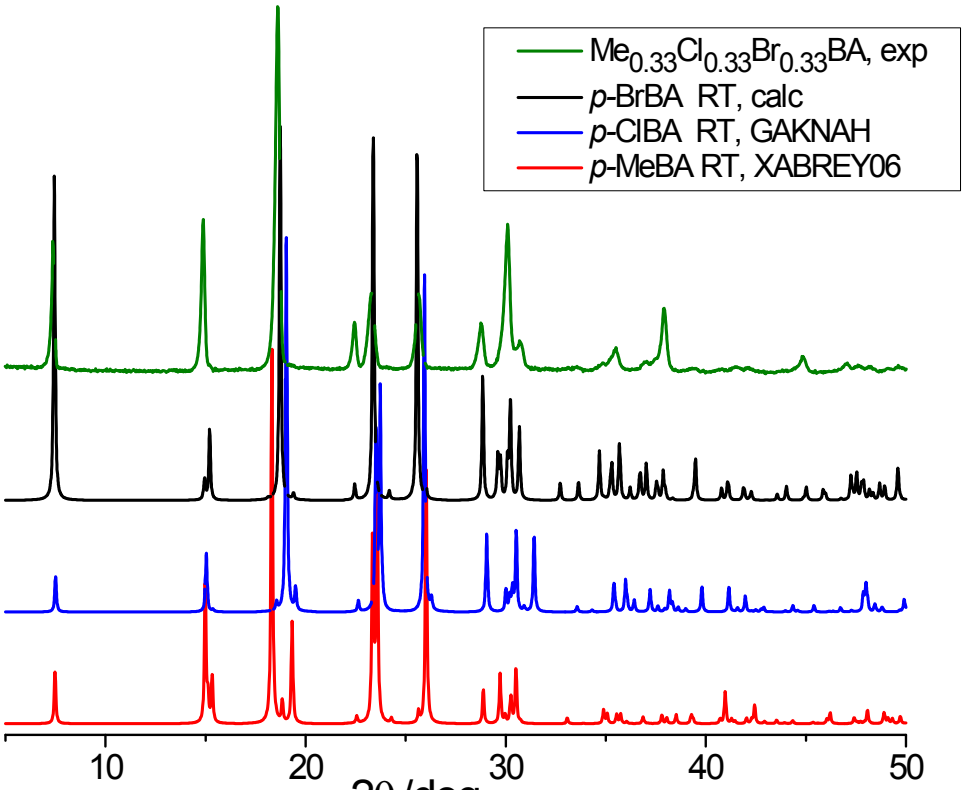

Fig. ESI-3. Comparison of the experimenatl X-ray powder pattern for the *p*-$MeBA_{0.33}ClBA_{0.33}BrBA_{0.33}$ solid solution with the patterns calculated from single crystal data for the Me/Cl/Br pure compounds.

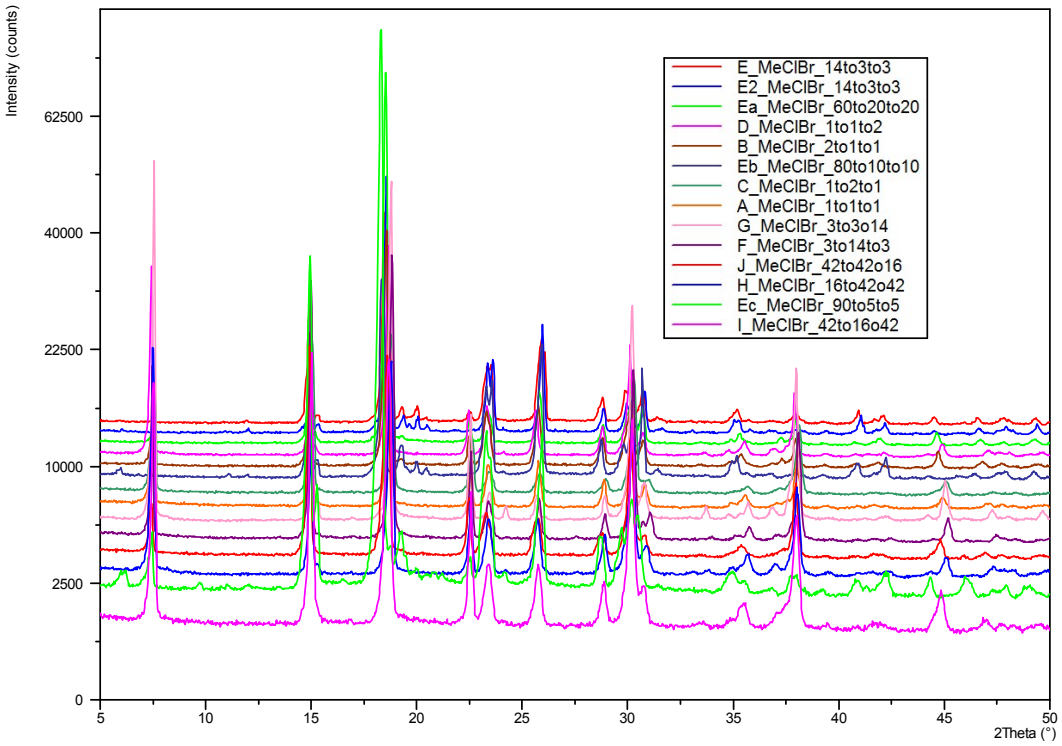

Fig. ESI-4. X-ray powder patterns of ternary solid solution of *p*-MeBA/*p*-ClBA/*p*-BrBA at varying molar ratios.

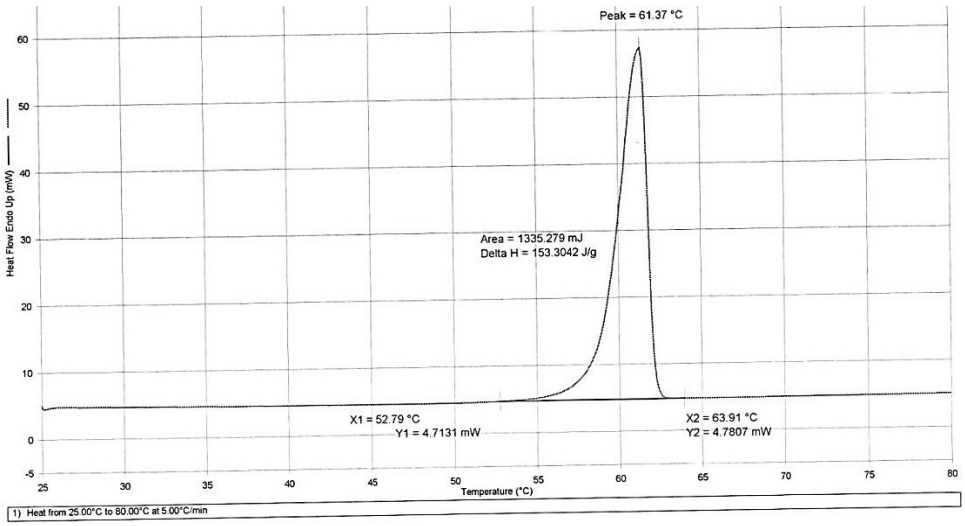

Fig. ESI-5. of *p*-MeBA II

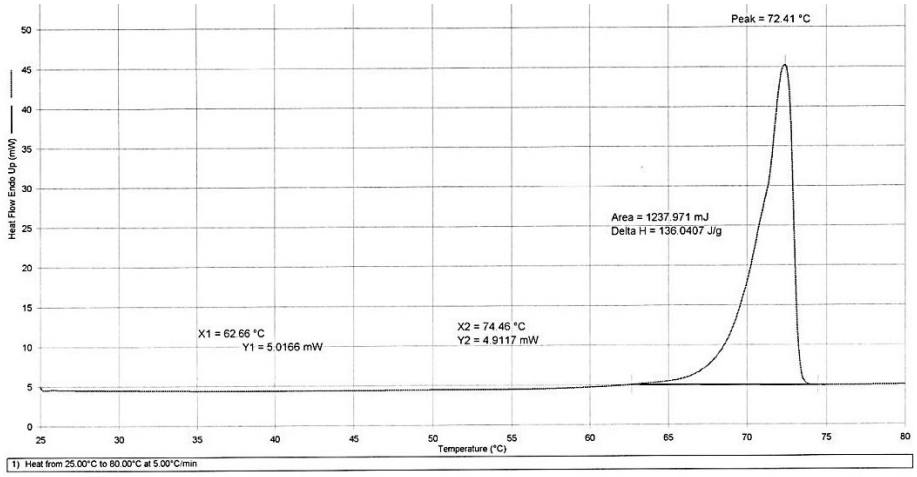

Fig. ESI-6 DSC of *p*-ClBA

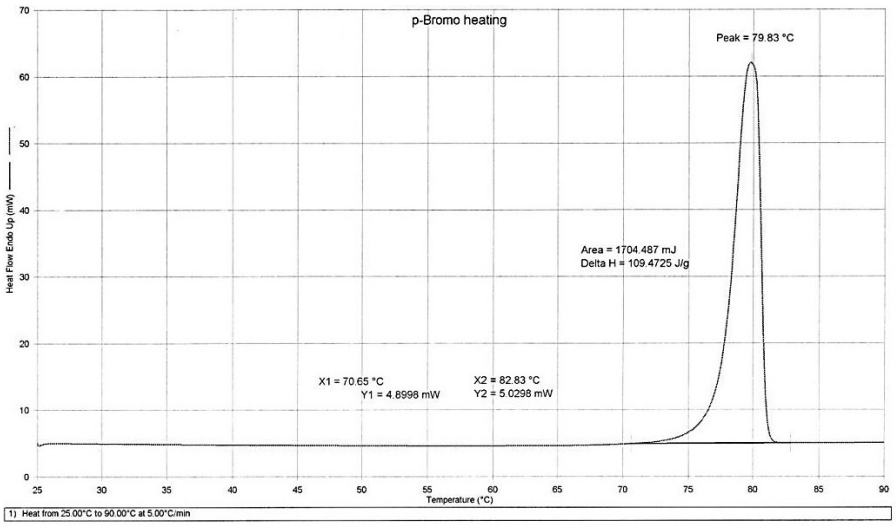

Fig. ESI-7. DSC of *p*-BrBA

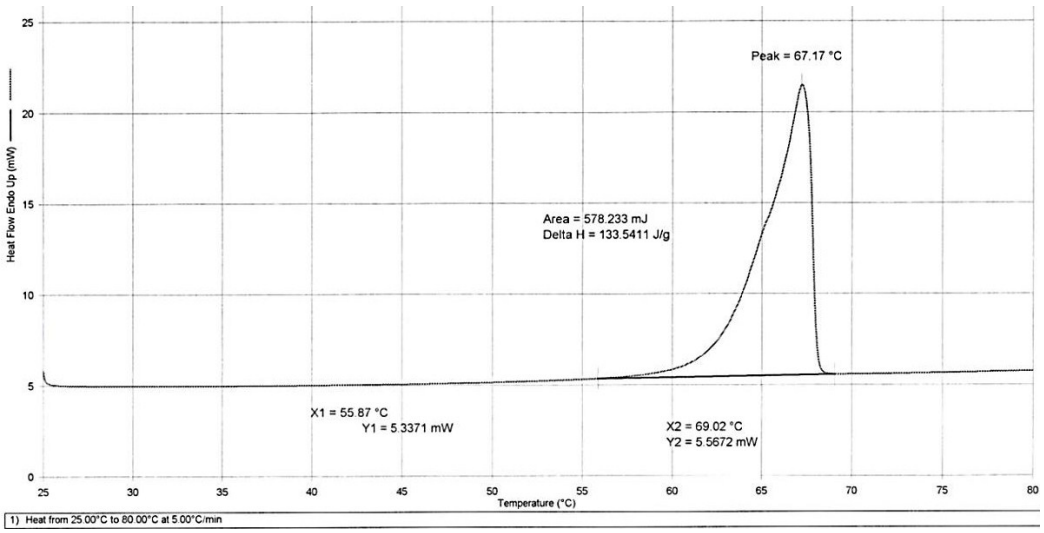

Fig. ESI-8. DSC trace (heating cycle) of the $MeBA_{0.1}ClBA_{0.9}$ solid solution obtained by co-melting.

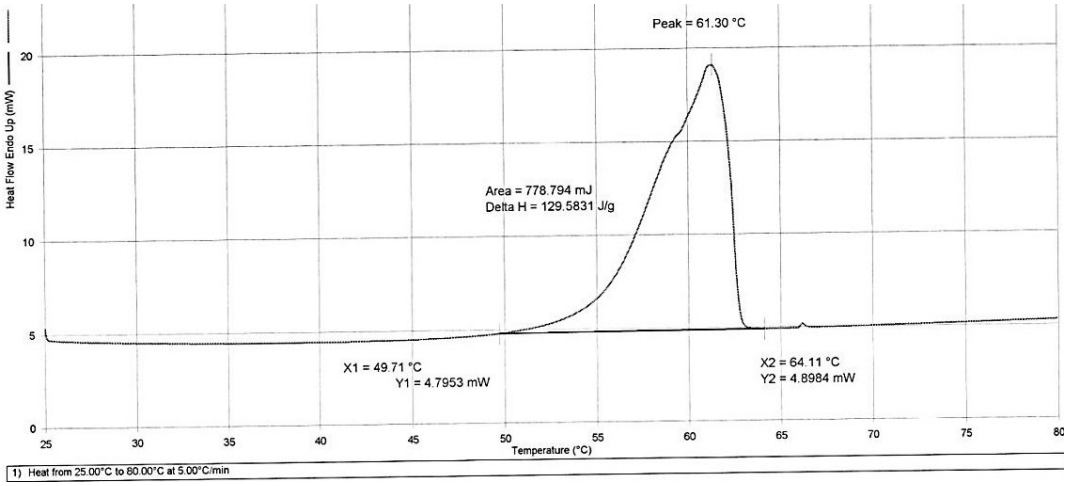

Fig. ESI-9. DSC trace (heating cycle) of the $MeBA_{0.25}ClBA_{0.75}$ solid solution obtained by co-melting.

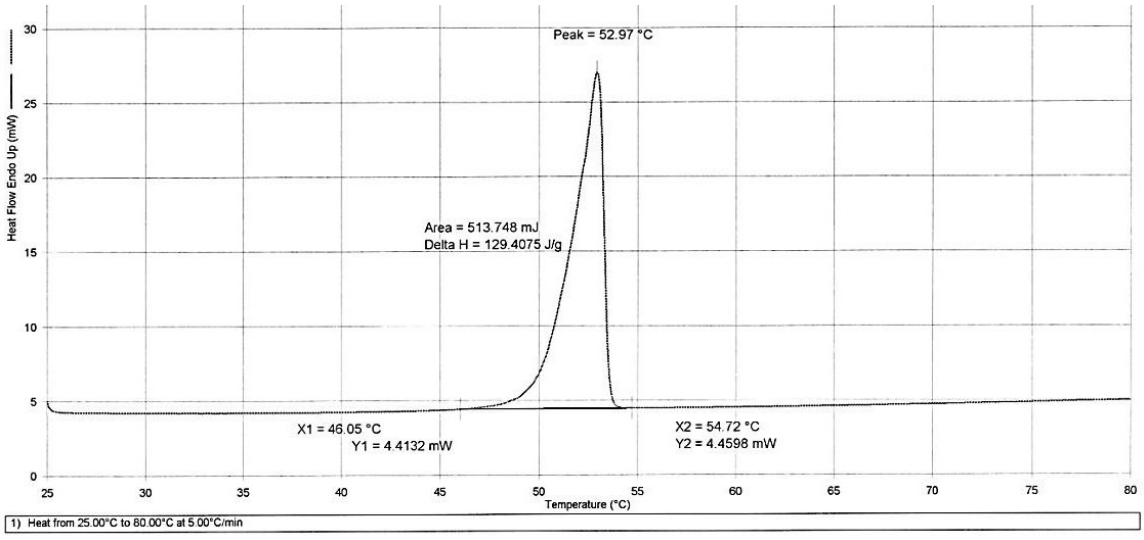

Fig. ESI-10. DSC trace (heating cycle) of the $MeBA_{0.5}ClBA_{0.5}$ solid solution obtained by co-melting.

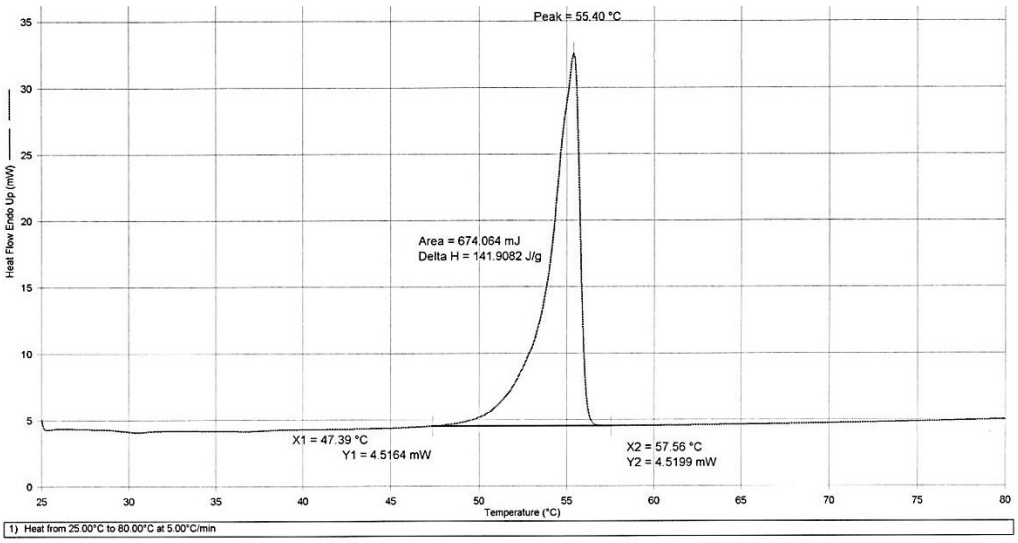

Fig. ESI-11. DSC trace (heating cycle) of the $MeBA_{0.75}ClBA_{0.25}$ solid solution obtained by co-melting.

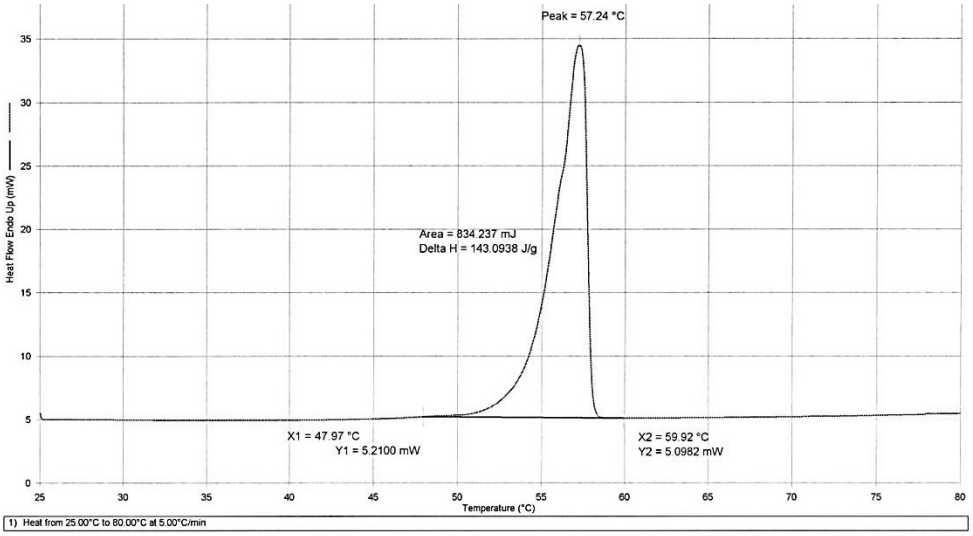

Fig. ESI-12. DSC trace (heating cycle) of the $MeBA_{0.9}ClBA_{0.1}$ solid solution obtained by co-melting.

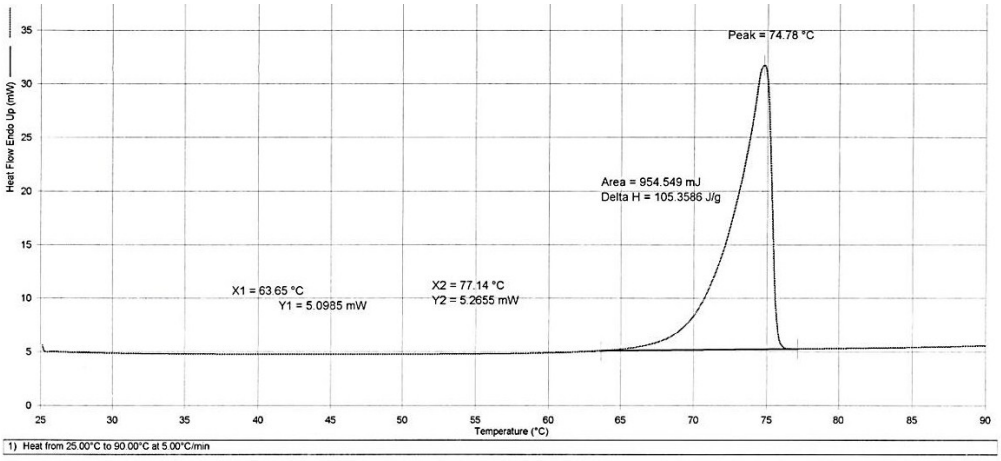

Fig. ESI-13. DSC trace (heating cycle) of the $MeBA_{0.1}BrBA_{0.9}$ solid solution obtained by co-melting.

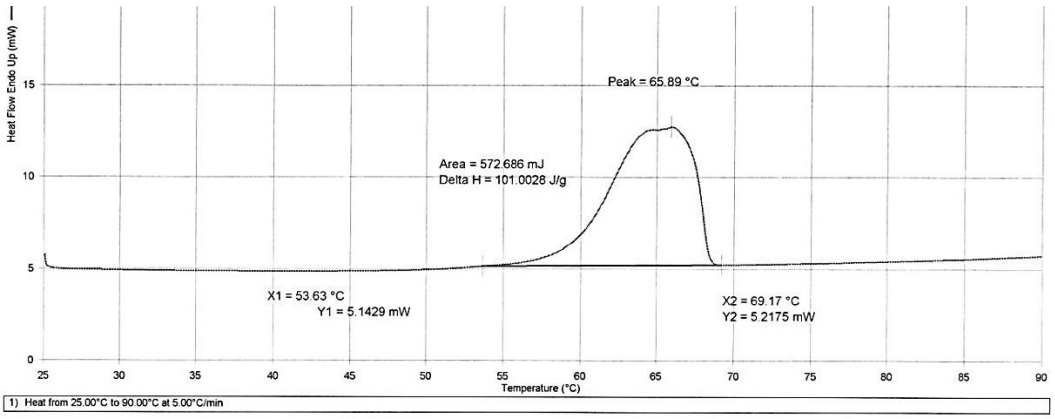

Fig. ESI-14. DSC trace (heating cycle) of the $MeBA_{0.25}BrBA_{0.75}$ solid solution obtained by co-melting.

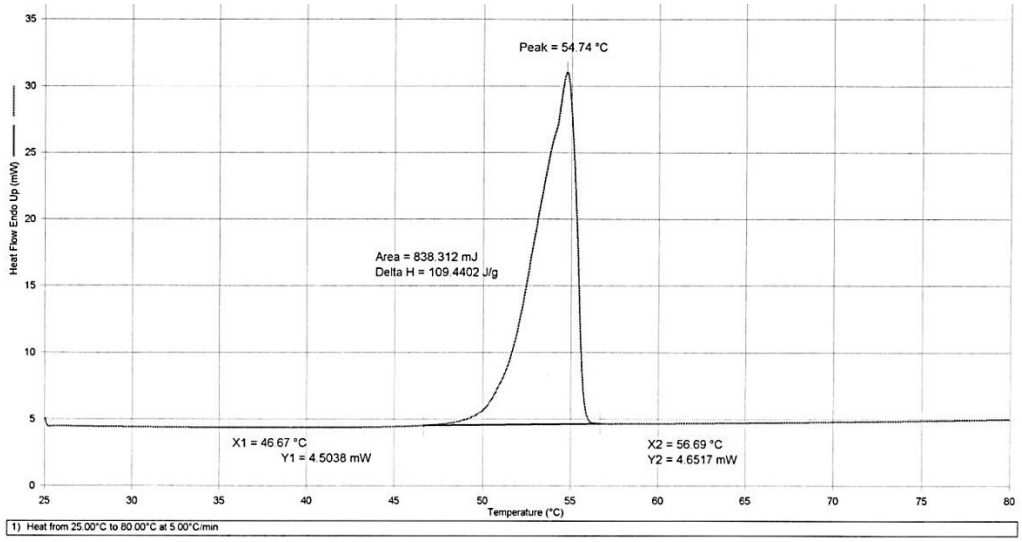

Fig. ESI-15. DSC trace (heating cycle) of the $MeBA_{0.5}BrBA_{0.5}$ solid solution obtained by co-melting.

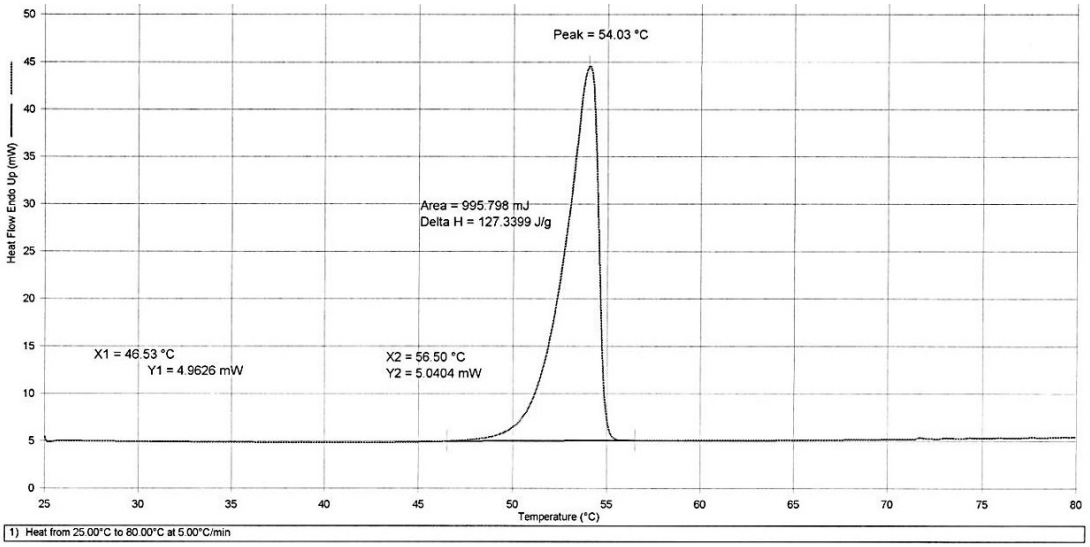

Fig. ESI-16. DSC trace (heating cycle) of the $MeBA_{0.75}BrBA_{0.25}$ solid solution obtained by co-melting.

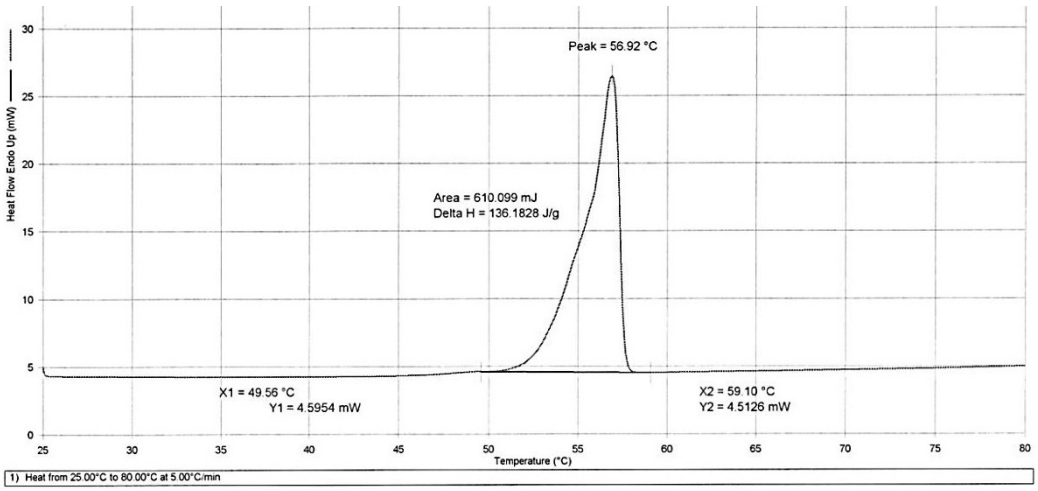

Fig. ESI-17. DSC trace (heating cycle) of the $MeBA_{0.9}BrBA_{0.1}$ solid solution obtained by co-melting.

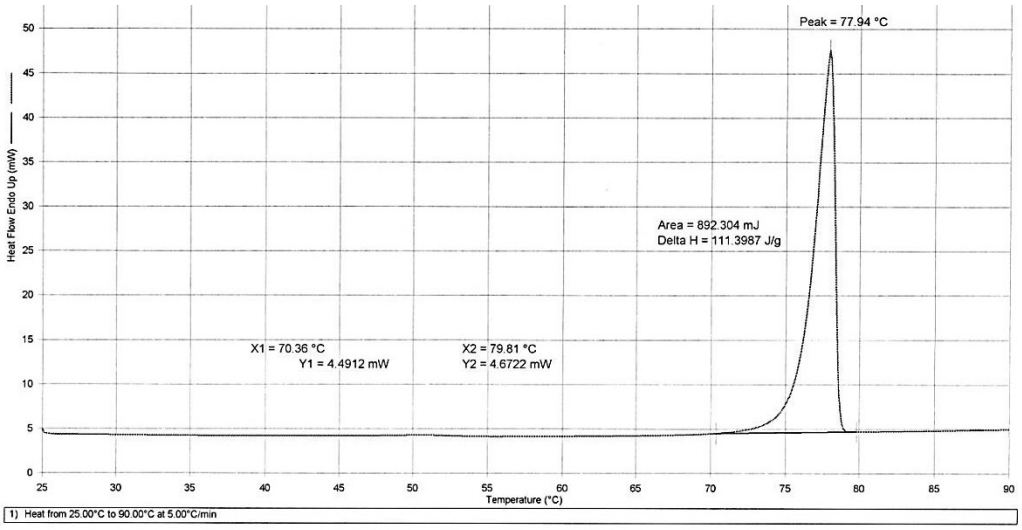

Fig. ESI-18. DSC trace (heating cycle) of the $ClBA_{0.1}BrBA_{0.9}$ solid solution obtained by co-melting.

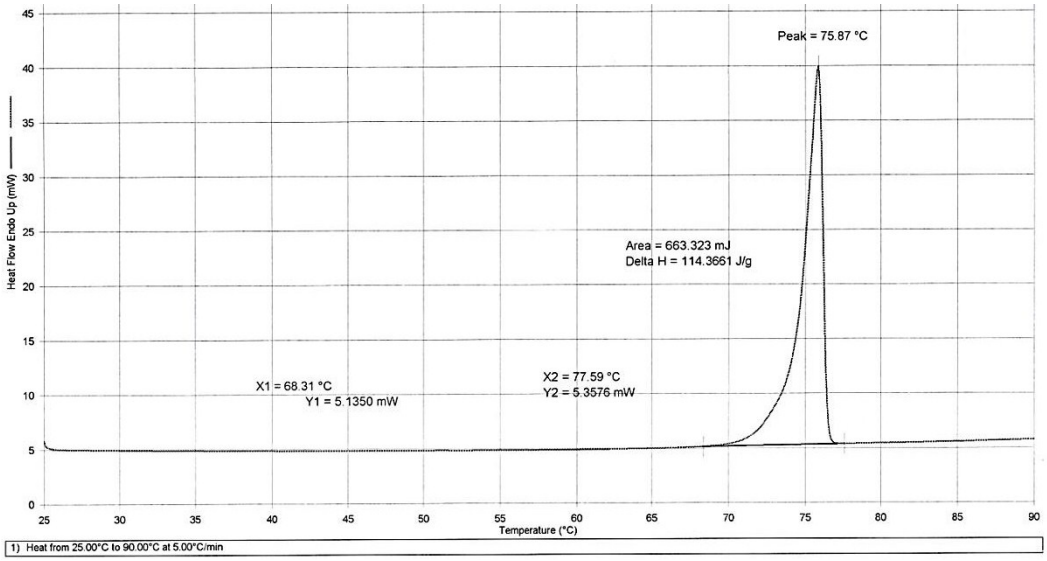

Fig. ESI-19. DSC trace (heating cycle) of the $ClBA_{0.25}BrBA_{0.75}$ solid solution obtained by co-melting.

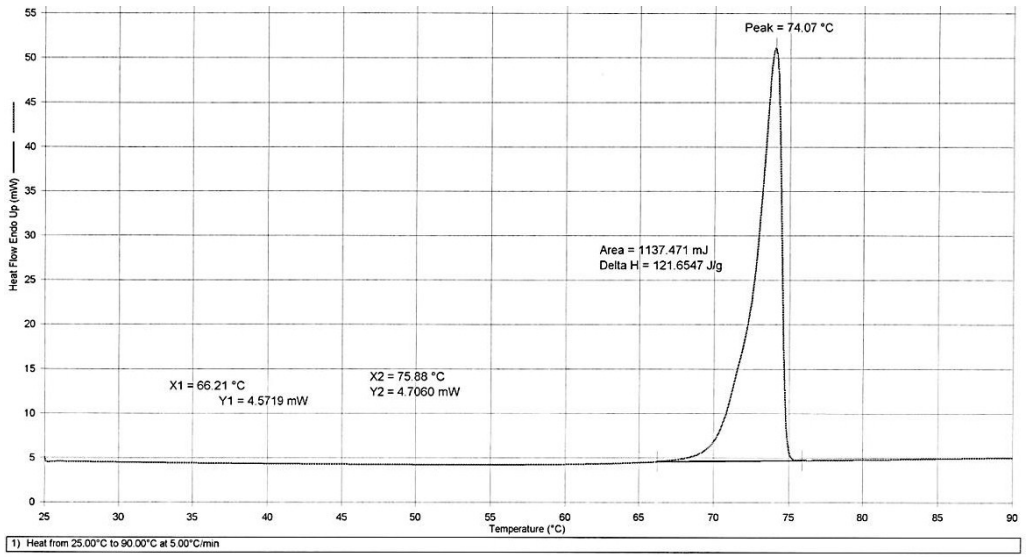

Fig. ESI-20. DSC trace (heating cycle) of the $ClBA_{0.5}BrBA_{0.5}$ solid solution obtained by co-melting.

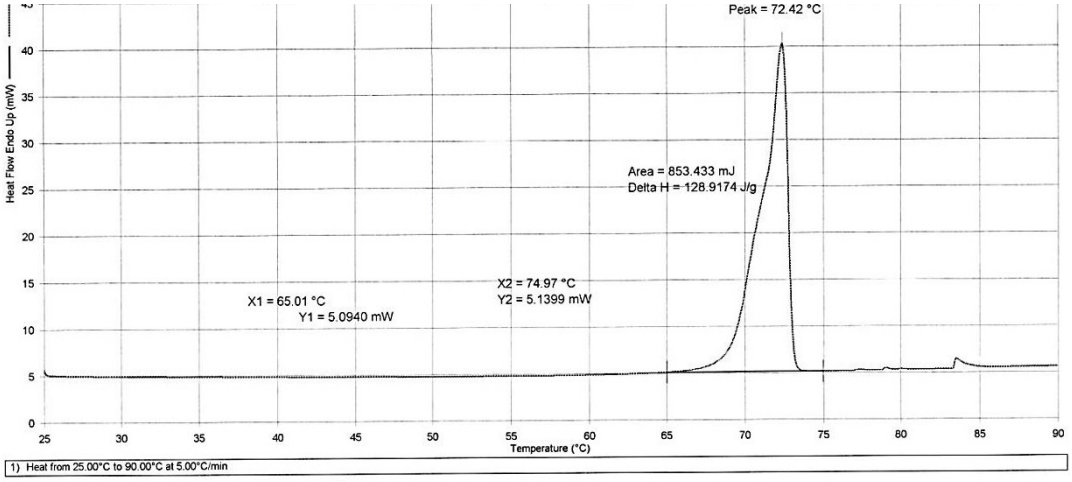

Fig. ESI-21. DSC trace (heating cycle) of the $ClBA_{0.75}BrBA_{0.25}$ solid solution obtained by co-melting.

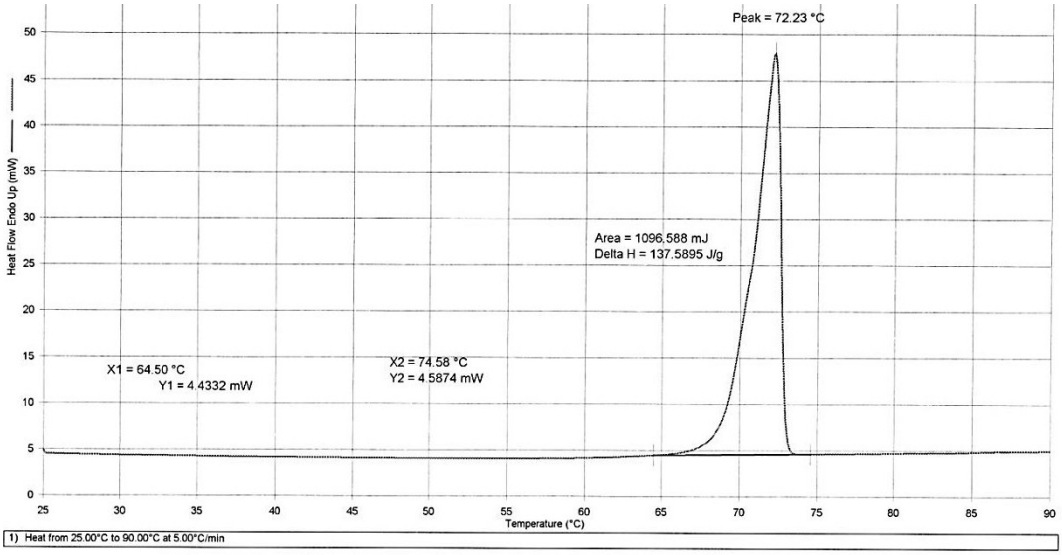

Fig. ESI-22. DSC trace (heating cycle) of the $ClBA_{0.9}BrBA_{0.1}$ solid solution obtained by co-melting.

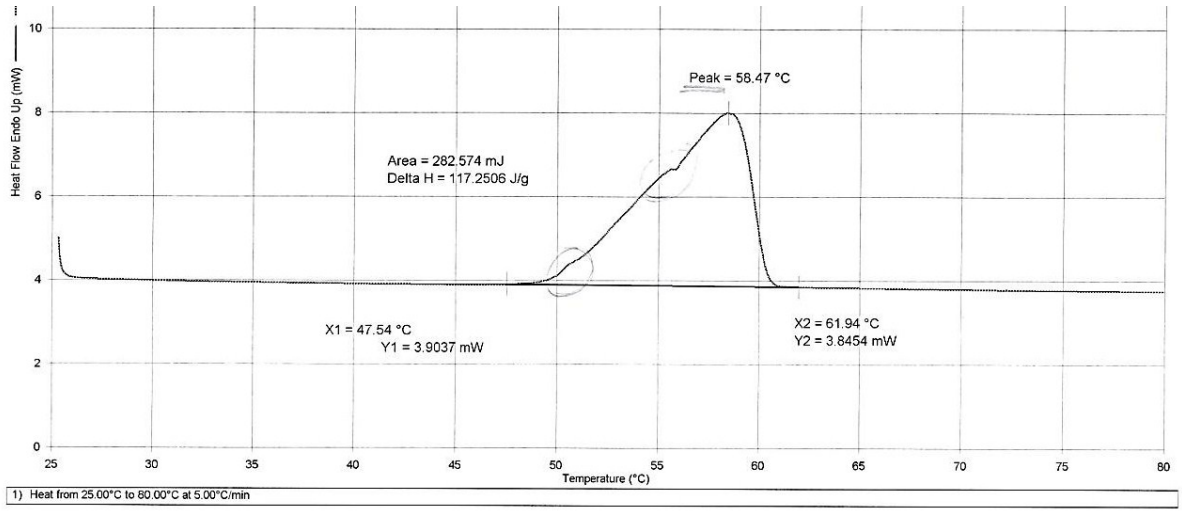

Fig. ESI-23. DSC trace (heating cycle, 5 °C min^{-1}) of the $MeBA_{0.33}ClBA_{0.33}BrBA_{0.33}$ solid solution obtained by co-melting.

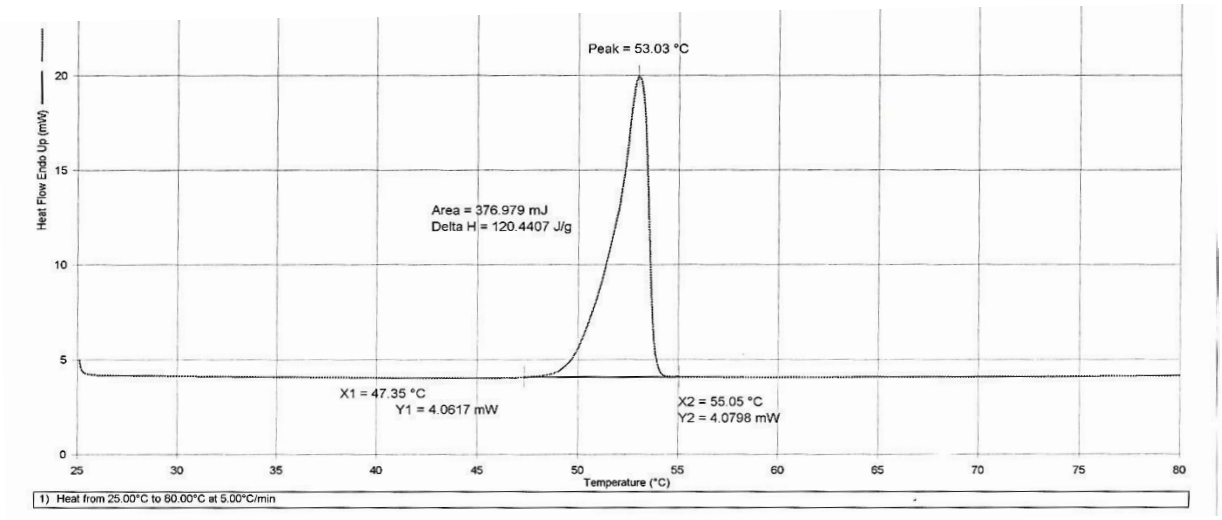

Fig. ESI-24. DSC trace (heating cycle) of the $MeBA_{0.50}ClBA_{0.25}BrBA_{0.25}$ solid solution obtained by co-melting.

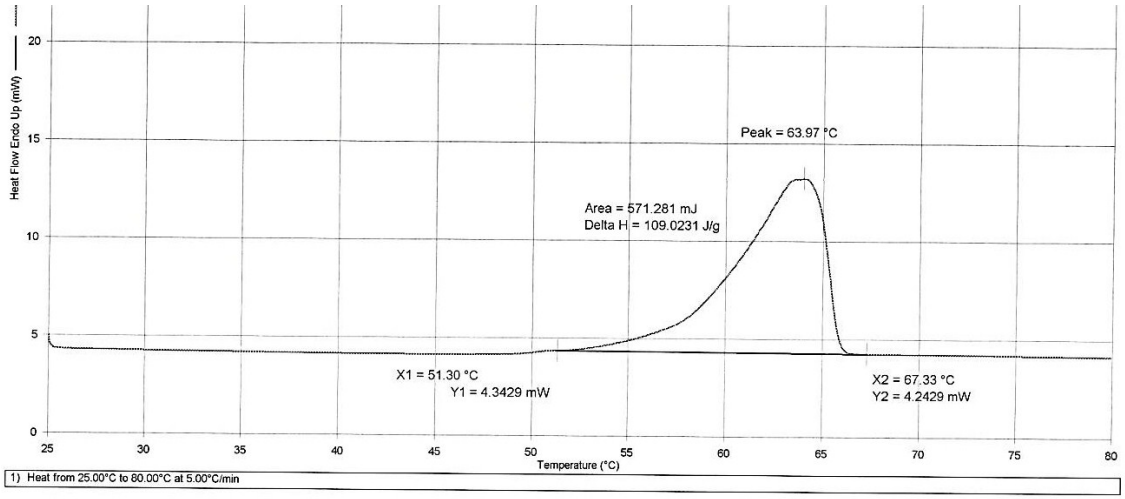

Fig. ESI-25. DSC trace (heating cycle) of the $MeBA_{0.25}ClBA_{0.25}BrBA_{0.50}$ solid solution obtained by co-melting.

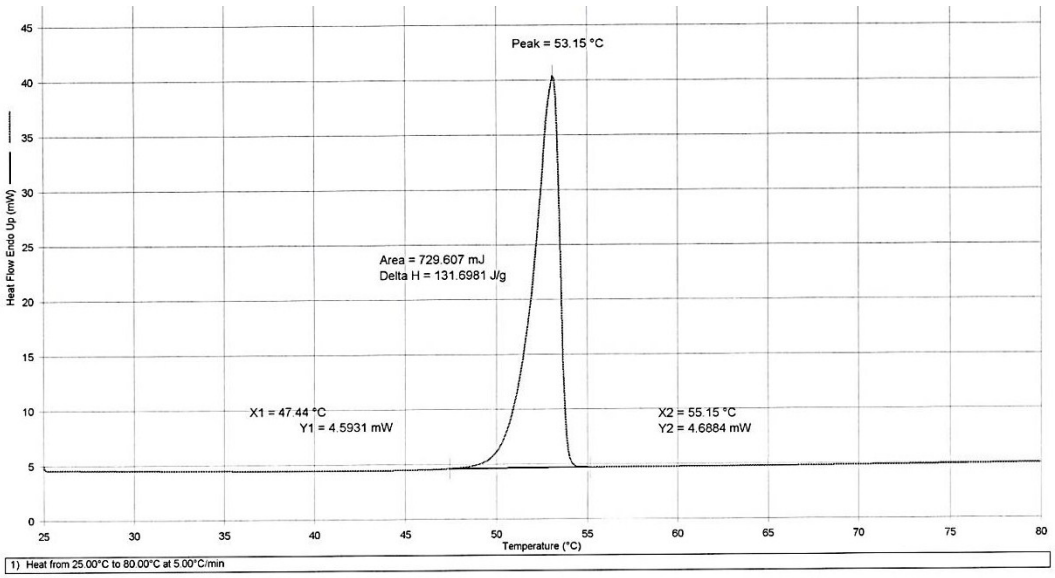

Fig. ESI-26. DSC trace (heating cycle) of the $MeBA_{0.70}ClBA_{0.15}BrBA_{0.15}$ solid solution obtained by co-melting.

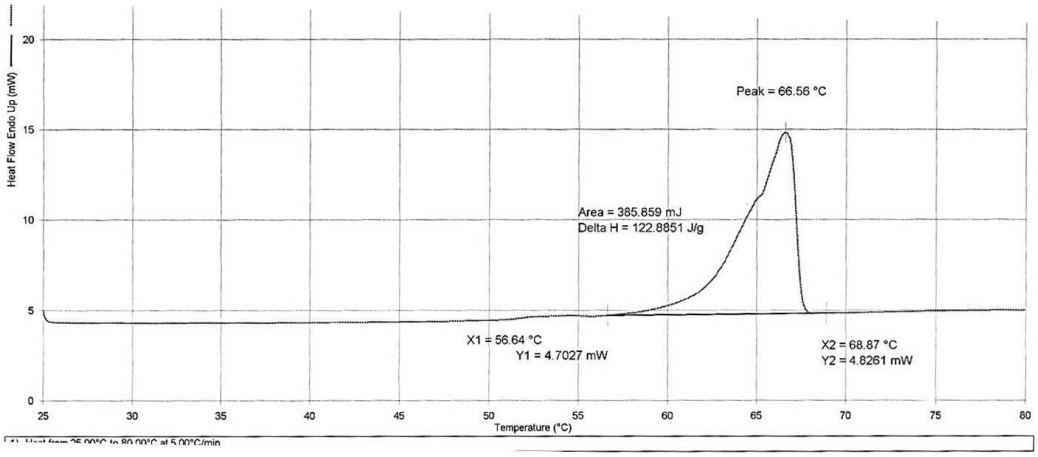

Fig. ESI-27. DSC trace (heating cycle) of the $MeBA_{0.15}ClBA_{0.70}BrBA_{0.15}$ solid solution obtained by co-melting.

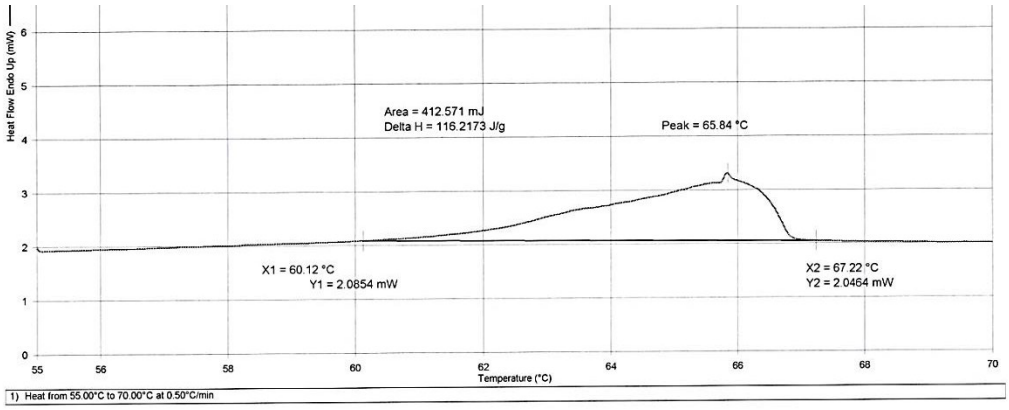

Fig. ESI-28. DSC trace (heating cycle, heating rate 0.5 °C min^{-1}) of the $MeBA_{0.15}ClBA_{0.70}BrBA_{0.15}$ solid solution obtained by co-melting. The lower heating rate was chosen to check for the possible presence of a second endothermic event before the melting temperature of the solid solution.

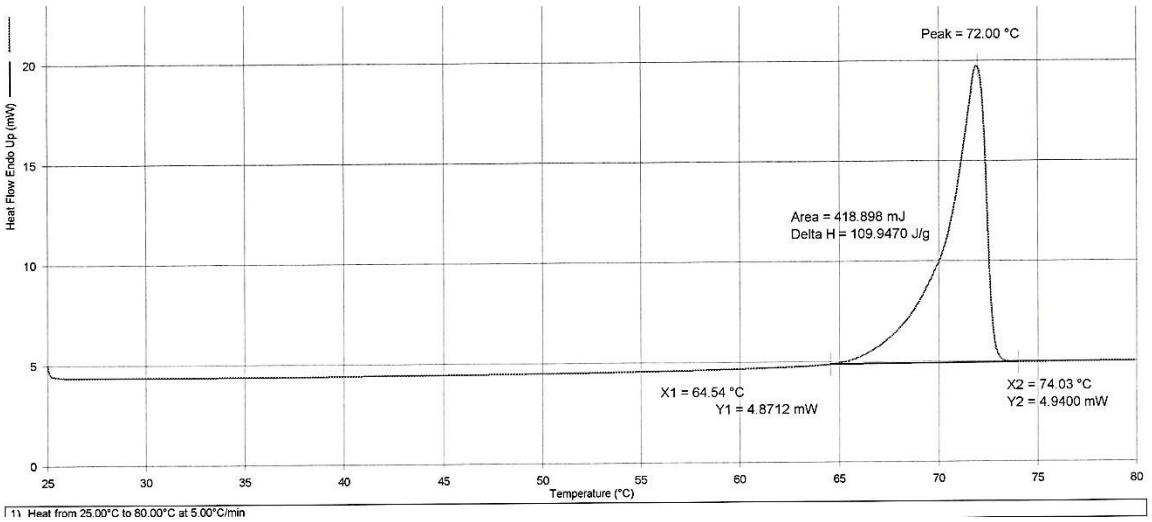

Fig. ESI-29. DSC trace (heating cycle) of the $MeBA_{0.15}ClBA_{0.15}BrBA_{0.70}$ solid solution obtained by co-melting.

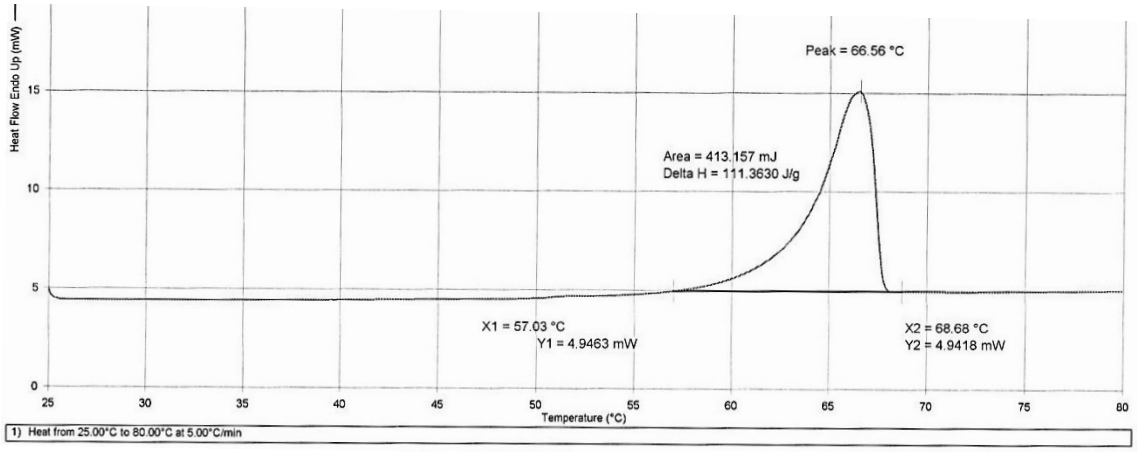

Fig. ESI-30. DSC trace (heating cycle) of the $MeBA_{0.16}ClBA_{0.42}BrBA_{0.42}$ solid solution obtained by co-melting.

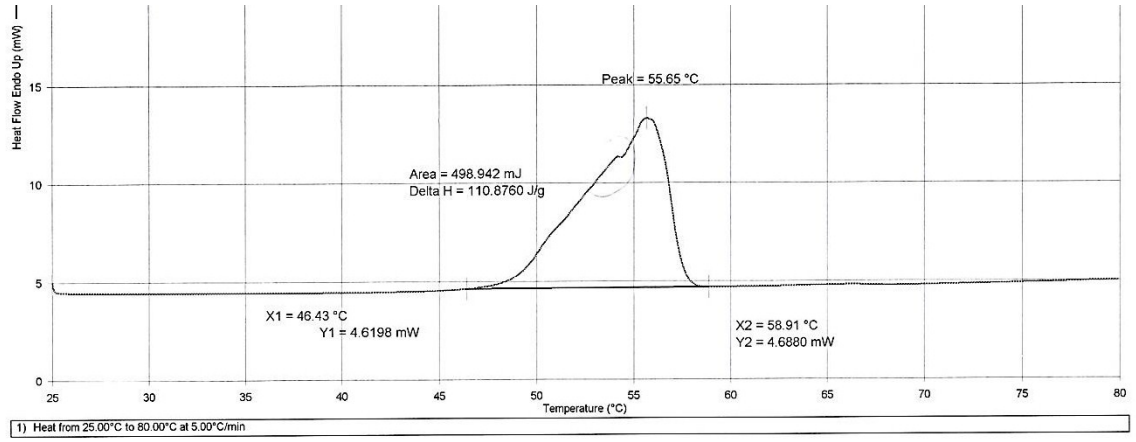

Fig. ESI-31. DSC trace (heating cycle) of the $MeBA_{0.42}ClBA_{0.16}BrBA_{0.16}$ solid solution obtained by co-melting.

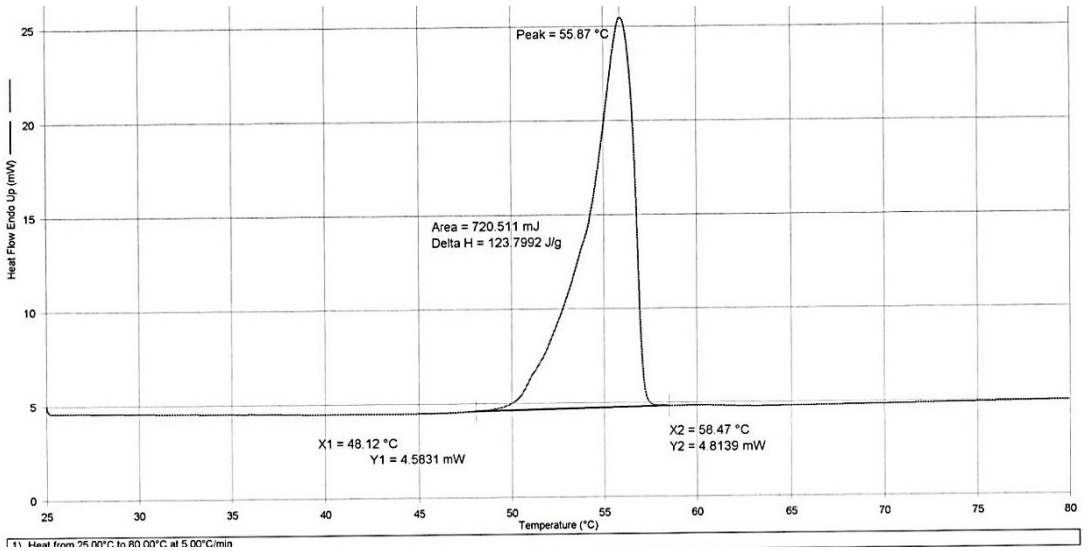

Fig. ESI-32. DSC trace (heating cycle) of the $MeBA_{0.42}ClBA_{0.42}BrBA_{0.16}$ solid solution obtained by co-melting.